Bloch k-selective resonant inelastic scattering of hard x rays at valence electrons of Ni in NiAl

H. Enkisch, A. Kaprolat, and W. Schülke
Institute of Physics, University of Dortmund, D-44221 Dortmund, Germany

M. H. Krisch and M. Lorenzen
ESRF, Boîte Postale 220, F 38043 Grenoble, France
(Received 18 March 1999)

We have measured x-ray fluorescence spectra from a stoichiometric NiAl single crystal after resonant excitation at the Ni *K* edge using synchrotron radiation. The shape of the spectra strongly depends on both excitation energy and scattering angle. This effect can be understood by considering a resonant inelastic-scattering process leading to a law of Bloch **k**-momentum conservation. We find clear evidence of this Bloch **k**-selection rule in the hard x-ray region. The measured spectra are in good agreement with calculated spectra based on a linearized augmented plane wave band-structure calculation. [S0163-1829(99)09735-0]

I. INTRODUCTION

Recent studies (Refs. 1–9) have shown that in the case of resonantly excited fluorescence emission from valence electrons the two-step model of absorption followed by emission breaks down. In this case the absorption and emission of a photon has to be treated as one single resonant inelastic-scattering process. Calculation of the respective scattering cross section gives rise to a law of Bloch **k**-momentum conservation that couples the emission process to the absorption process of the incident photon. As a result, it is possible to investigate the density of states (DOS) of the valence bands Bloch **k** selectively. Moreover, due to the resonant excitation, this technique is element specific and symmetry selective whereby more specific information can be acquired than by other techniques like photoemission spectroscopy (PES) and angle-resolved photoemission spectroscopy (ARPES) (Ref. 10), which are well-established methods to measure the total DOS and the band structure, respectively.

Previous investigations of Bloch **k**-selective resonant inelastic scattering (Refs. 1–9) were restricted to the soft x-ray region up to about 2 keV. First, evidence for the validity of Bloch **k**-momentum conservation in the hard x-ray region has been found by Kaprolat and Schülke.[11] In this paper we present a systematic study at the *K* edge of Ni in NiAl. The experimental data are in good agreement with calculated fluorescence spectra based on linearized augmented plane wave (LAPW) band-structure calculations. Our results clearly demonstrate the validity of Bloch **k**-momentum conservation as well as the element and symmetry selectivity of this technique in the hard x-ray region.

II. THEORY

The double-differential scattering cross section (DDSCS) for resonant inelastic x-ray scattering (RIXS) requires treatment up to second order perturbation theory of the $\mathbf{p}\cdot\mathbf{A}$ term of the interaction Hamiltonian H_{int}, which describes the interaction of an electron with a photon field. This leads to the Kramers-Heisenberg formula:[12]

$$\frac{d^2\sigma}{d\omega_2 d\Omega}\sim\sum_f\left|\sum_m\frac{\langle f|\mathbf{p}\cdot\mathbf{A}|m\rangle\langle m|\mathbf{p}\cdot\mathbf{A}|i\rangle}{E_m-E_i-\hbar\omega_1-i\Gamma_m/2}\right|^2\times\delta(E_f-E_i-\hbar\omega_1+\hbar\omega_2),\tag{2.1}$$

where $|i\rangle$ is the initial state that corresponds to the ground state of the system, $|m\rangle$ stands for the intermediate state after absorption of a photon and excitation of an electron from a core state into the conduction band, and $|f\rangle$ is the final state after reoccupation of the core state by a valence electron and emission of the fluorescence photon. $E_{i,m,f}$ are the respective energies of the electron states, $\hbar\omega_1$ and $\hbar\omega_2$ are the energies of the incident and the scattered photon, respectively, and Γ_m is the energy width of the intermediate state due to its finite lifetime.

A single-particle treatment of Eq. (2.1) was given by Ma[13] resulting in

$$\frac{d^2\sigma}{d\omega_2 d\Omega}\sim\sum_{\mathbf{k}_1,\mathbf{k}_2}|M_{\mathbf{k}_1,c}|^2\delta(E(\mathbf{k}_1)-E_c-\hbar\omega_1)\times\delta_{\mathbf{G},(\mathbf{q}_1-\mathbf{q}_2-\mathbf{k}_1+\mathbf{k}_2)}|M_{\mathbf{k}_2,c}|^2\times\delta(E(\mathbf{k}_2)-E_c-\hbar\omega_2).\tag{2.2}$$

Therein $\mathbf{k}_1$ and $\mathbf{k}_2$ denote the Bloch **k** vectors of the conduction- and valence-band states, respectively, involved in the scattering process, $\mathbf{q}_1$ and $\mathbf{q}_2$ are the wave vectors of the incident and the emitted photon, respectively, and $M_{\mathbf{k}_1,c}$ and $M_{\mathbf{k}_2,c}$ denote the transition matrix elements of the absorption and the emission process, respectively. The use of the index c instead of $\mathbf{k}_c$ for the core states indicates that these are **k** independent due to their localization in direct space. If the energy transfer is small compared to the incident energy, the momentum transfer $\hbar\mathbf{q}=\hbar(\mathbf{q}_1-\mathbf{q}_2)$ is related to the scattering angle Θ by $|\mathbf{q}|\approx 2|\mathbf{q}_1|\sin\Theta/2$.

The use of the conventional two-step model, that is treating the $\mathbf{p}\cdot\mathbf{A}$ term of H_{int} in first-order perturbation theory for both the absorption and the emission process separately, instead of the above one-step scheme, would yield just the

 ©1999 The American Physical Society

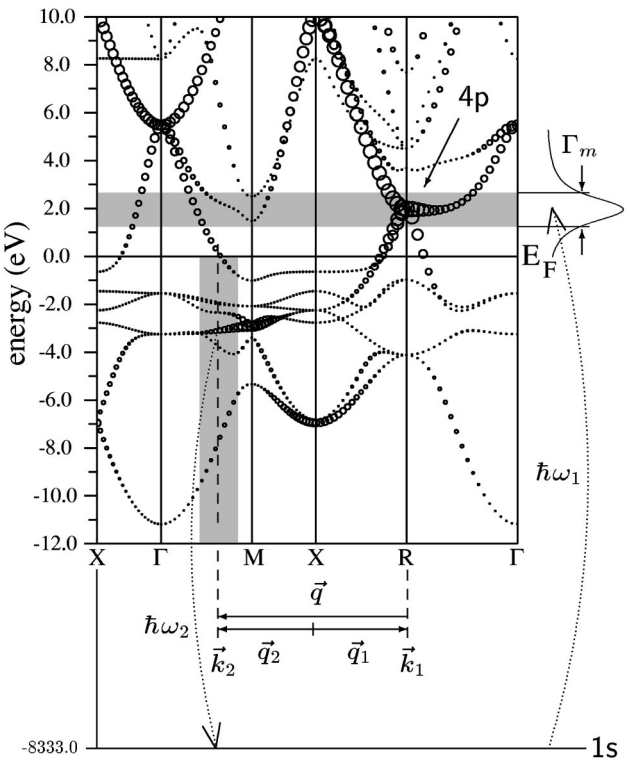

FIG. 1. Schematic of the resonant inelastic-scattering process from valence electrons of Ni in NiAl. The radii of the circles are proportional to the Ni-p partial charge of the respective state.

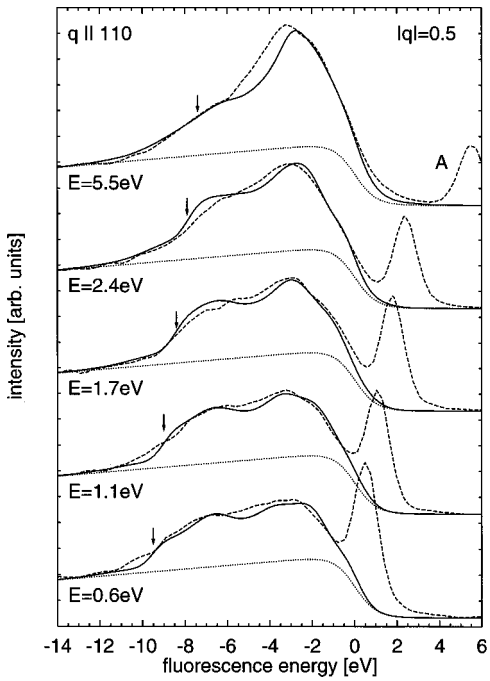

FIG. 2. Measured (dashed lines) and calculated (solid lines) spectra with constant momentum transfer together with the estimated shakeup satellite (dotted line). The primary energy $E=\hbar\omega_1$ and the fluorescence energy $\hbar\omega_2$ are given with a zero at the Ni 1s binding energy (8333 eV). $|\mathbf{q}|$ is given in units of $|\langle 110\rangle|2\pi/a$. The narrow peak labeled with A dispersing from 0.6 eV to 5.5 eV is due to quasielastic scattering. To make the calculated spectra comparable to the experiment, we show the sum of the calculated spectra and the estimated satellite.

same result except for the Kronecker delta, which expresses the law of Bloch **k**-momentum conservation:

$$\delta_{\mathbf{G},(\mathbf{q}_1-\mathbf{q}_2-\mathbf{k}_1+\mathbf{k}_2)}. \tag{2.3}$$

It states that the momentum transferred to the system by the scattered photon must be equal to the difference of the Bloch **k** vectors $\mathbf{k}_1$ and $\mathbf{k}_2$ of the two electrons involved in the scattering process modulo any reciprocal-lattice vector **G**.

Based on Eq. (2.2), one can explain the dependence of the shape of the fluorescence spectra on the energy $\hbar\omega_1$ of the incident photon and on the momentum transfer **q** (see Fig. 1). The first δ function states the conservation of energy during the absorption of the incoming photon with energy $\hbar\omega_1$. It determines the possible energy eigenvalues the excited electron can occupy. Via the conduction-band structure, the first δ function also fixes the respective Bloch **k** vectors $\mathbf{k}_1$. Via the law of Bloch **k**-momentum conservation [Eq. (2.3)], the Bloch **k** vectors $\mathbf{k}_2$ of the valence states involved in the scattering process depend on **q** and $\mathbf{k}_1$ and hence on $\hbar\omega_1$. Finally, the second δ function determines the energy $\hbar\omega_2$ of the emitted photon. As a result, only valence states with a Bloch **k** vector equal to $\mathbf{k}_2$ can refill the core hole. Therefore, only a small part of the Brillouin zone is contributing to the emission process, and consequently, only a part of the DOS is reflected in the fluorescence spectrum. This restricted DOS is determined by $\hbar\omega_1$ and **q**.

Due to the dispersion of the conduction and valence bands, the fluorescence spectrum changes shape if either $\hbar\omega_1$ or **q** are varied. Moreover, by fixing $\hbar\omega_1$ and therefore the $\mathbf{k}_1$-values and by changing **q**, one can scan the emission points $\mathbf{k}_2$ within the irreducible wedge of the first Brillouin zone allowing one to trace dispersive valence bands.

Because of the resonant nature of the excitation, that is the participation of a core state, this technique is element specific. Additionally, certain symmetry selection rules, arising from the matrix elements $M_{\mathbf{k}_1,c}$ and $M_{\mathbf{k}_2,c}$, must be obeyed. Because of the dominance of dipole transitions one can, for example, investigate the $4p$ valence states of Ni if one chooses the incident energy close to the K edge of Ni. As a result, one can trace dispersive bands of certain symmetry originating from a certain element in the sample.

Nevertheless, the direct interconnection of $\mathbf{k}_1$ and $\mathbf{k}_2$ via the law of momentum conservation [Eq. (2.3)], sometimes called the coherence of the scattering process,[13] can be disturbed by relaxation of the intermediate state, i.e., by interaction with phonons[14] and excitonic excitations.[15] The use of hard x rays has the advantage that the lifetime of the intermediate state after excitation of a core state with a large binding energy is short and that therefore no phonon relaxation can take place. Moreover, hard x rays show no surface sensitivity, and therefore, only bulk properties influence the scattering process.

However, the most important advantage of hard x-ray over soft x-ray RIXS arises from the larger magnitude of the photon wave vector, which is large compared to the first Brillouin zone. Therefore, the momentum transfer **q** is not restricted by experimental conditions but can be varied freely allowing one to scan the whole first Brillouin zone without

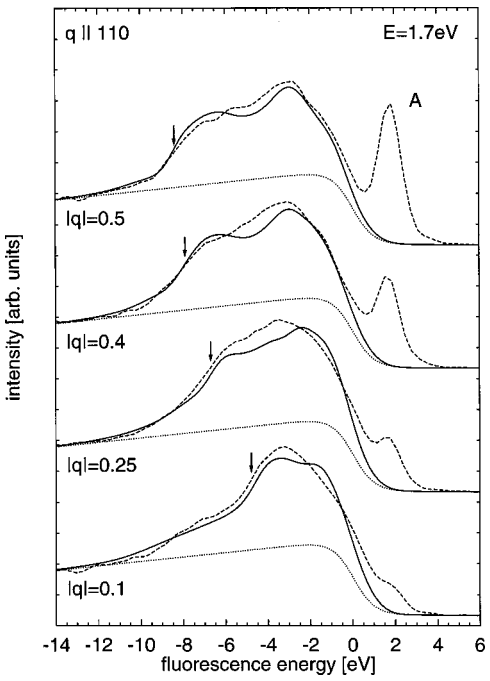

FIG. 3. Measured (dashed lines) and calculated (solid lines) spectra with constant primary energy at $E_{\mathrm{edge}}+1.7$ eV together with the estimated shakeup satellite (dotted line). Units are as in Fig. 2.

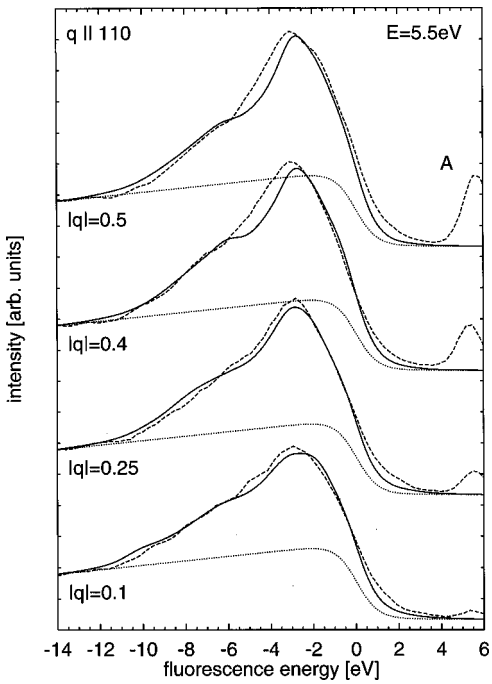

FIG. 4. Measured (dashed lines) and calculated (solid lines) spectra with constant primary energy at $E_{\mathrm{edge}}+5.5$ eV together with the estimated shakeup satellite (dotted line). Units are as in Fig. 2.

changing the primary energy. In the case of soft x-ray RIXS (since $|\mathbf{q}|\ll$any reciprocal lattice vector $|\mathbf{G}|$ and therefore $\mathbf{k}_1=\mathbf{k}_2$), the variation of the primary energy is the only way to scan the Brillouin zone. Nevertheless, in some very special cases such as SiC, a direct and quantitative measurement of the band structure using soft x-ray RIXS (Ref. 8) is possible, making use of the isotropic parabolic conduction bands of SiC.

However, a direct reconstruction of the valence-band structure out of RIXS data is impossible in general, since firstly the $\mathbf{k}_2$ points that contribute to one single fluorescence spectrum are always distributed over the whole first Brillouin zone, and secondly one needs to know the dispersion of the conduction bands.

To make full use of the information that is contained redundantly in a set of spectra, one would need to perform a self-consistent iterative reconstruction procedure that modifies an initial band structure to give the best agreement between calculated and measured spectra. In this context the possibility to vary $\mathbf{q}$ leading to a variation of the $\mathbf{k}_2$ points involved gives an additional degree of freedom, being a clear advantage of hard x-ray RIXS.

III. EXPERIMENT

To prove the element selectivity, we chose a single-crystal sample of the ordered stoichiometric alloy Ni_1Al_1, using excitation energies $\hbar\omega_1$ close to the Ni K edge. Moreover, the difficulties related to core excitons[15] are not present in this metallic sample. In addition, this sample has a conduction-band structure that allows one to select a relatively limited number of Bloch $\mathbf{k}$ points to contribute to absorption and emission.

The measurements have been performed at the beamline ID28 at the ESRF using a 1-m spherical crystal Rowland spectrometer with an energy resolution of about 0.5 eV. The incident radiation was monochromatized to about 8330 eV by a Si 111 double crystal monochromator and an additional Si 333 channel cut crystal. The full width at half maximum (FWHM) of the incident energy resolution was set to 0.85 eV resulting in an overall experimental resolution of 1.0 eV FWHM. Fluorescence spectra were measured for a set of four $\mathbf{q}$ values parallel to the 110 axis and five different primary energies $\hbar\omega_1$ for each $\mathbf{q}$. Series of measured spectra for fixed $\mathbf{q}$ and for fixed $\hbar\omega_1$ are shown in Figs. 2, 3, and 4, respectively. The experimentally chosen absolute values of $\mathbf{q}$ were of 0.1, 0.25, 0.4, and 0.5 in units of $|\langle 110\rangle|\cdot 2\pi/a$, a being the lattice constant, whereas the excitation energy $\hbar\omega_1$ for each $\mathbf{q}$ was set to 0.6, 1.1, 1.7, 2.4, and 5.5 eV above the $1s$ binding energy of Ni.

Inherent to this technique is the fact that the valence emission spectra lie on top of the so-called shakeup satellite to the valence line, sometimes described as a radiative Auger effect,[16,17] being the excitation of another valence electron into the conduction band during the emission process resulting in an energy loss of the emitted photon. The minimal energy loss of this process is zero whereas the maximum energy loss is not limited. Therefore, the shakeup satellite shows a steep drop on its high-energy side coincident with the binding energy of the $1s$ electron and a slowly decreasing tail on its low-energy side as indicated in Figs. 2–4. We have to emphasize that the satellite shown consists of a linear function multiplied by a Fermi function with a width of 2.2 eV. We chose this model because, to our knowledge, the satellite behavior in this energy regime has not yet been calculated and cannot be measured independently.

The calculated resonant emission spectra, following the scheme described above, are based on a LAPW band-

structure calculation using the WIEN97 package.[18] The energy eigenvalues and the partial charges at 9139 **k** points in the irreducible wedge of the first Brillouin zone were used. Furthermore, the finite-energy resolution of both the monochromator and the spectrometer together with the lifetime broadening of the core state were taken into account. Additionally, we have accounted for self-absorption effects and for the energy dependence of the dipole matrix elements of the Ni-1*s* to Ni-4*p* transition. From Ge valence fluorescence spectra, where emission lines from the 4*p* and 3*d* orbitals are nicely separated, we estimate the contribution of the quadrupolar Ni-3*d* to Ni-1*s* transition to be 2 orders of magnitude smaller than the dipolar transition. For the quadrupolar transition, no energy dependent matrix elements have been used.

As can be seen from Figs. 2–4, there is considerable agreement between the measured and the calculated spectra. Despite the fact that the Bloch **k**-space resolution (via the conduction-band structure) is limited by the energy width of the intermediate state ($\Gamma \approx 1.3$ eV), the shape of the fluorescence spectra changes significantly with both the primary energy (Fig. 2) and the momentum transfer (Fig. 3). A dispersion of the low-energy shoulder in both cases marked by the arrows is clearly visible. Also the growth of the main peak at -3 eV with increasing primary energy is nicely reproduced in the calculated spectra (Fig. 2).

These changes can be easily explained by distinct features of the electronic band structure (see Fig. 1). If $\hbar\omega = E_{1s} + 1.7$ eV (Fig. 3), the possible $\mathbf{k}_1$ vectors are distributed around the *R* point. With increasing $|\mathbf{q}|$, the $\mathbf{k}_2$ are shifted parallel to the 110 direction from the *R* point to the *X* point, and consequently, the lowest band with *p* character around *X* causes the dispersing shoulder. Similarly in Fig. 2 the growth of the main peak at -3 eV is originating from the *p* states around *M*.

Even though the spectra of the series with $\hbar\omega = E_{1s} + 5.5$ eV (Fig. 4) are different from the spectra at $\hbar\omega = E_{1s} + 1.7$ eV, the changes with varying **q** are not as large as in the series at lower energy. From the good agreement with the calculated spectra, we conclude that this decreasing **q** sensitivity is exclusively a band-structure effect. The reduced **q** sensitivity gives evidence of an increased number and a more widely spread distribution of $\mathbf{k}_2$ points that contribute to the emission, originating from the increased number of bands in that energy region. This is *not* a loss of coherence in the sense of Ref. 13 but again a proof of the validity of the Bloch **k** selectivity in the hard x-ray regime.

Calculated emission spectra from Al-3*p* orbitals show no agreement with the experiment. From this we conclude that for resonant inelastic scattering from valence electrons the element selectivity holds.

IV. CONCLUSION

In summary, we have investigated resonant inelastic scattering of hard x rays from valence electrons of Ni in NiAl using four different values of momentum transfer **q** and for each **q** five different energies $\hbar\omega_1$ of the incident radiation. These measurements reveal that the two-step model fails and that the treatment as one single resonant scattering process is in good agreement with the experiment. The validity of the Bloch **k**-momentum conservation as well as the selectivity of the scattering process to the element and to the symmetry of the orbitals have been shown. Band-structure effects are clearly visible as expected.

ACKNOWLEDGMENTS

This work was funded by the German Federal Ministry of Education and Research under Contract No. 05 SC8PEA4. One of us (A.K.) is indebted to the Deutsche Forschungsgemeinschaft for financial support. We acknowledge D. Gambetti, B. Gorges, K. Martel, and O.F. Ribois for their technical assistance in construction and commissioning of beamline ID28 at the ESRF.

[1] J-E. Rubensson, D. Meuller, R. Shuker, D. L. Ederer, C. H. Zhang, J. Jia, and T. A. Callcott, Phys. Rev. Lett. **64**, 1047 (1990).

[2] Y. Ma, N. Wassdahl, P. Skytt, J. Guo, J. Nordgren, P. D. Johnson, J-E. Rubensson, T. Boske, W. Eberhardt, and S. D. Kevan, Phys. Rev. Lett. **69**, 2598 (1992).

[3] K. E. Miyano, D. L. Ederer, T. A. Callcott, W. L. O'Brine, J. J. Jia, L. Zhou, Q.-Y. Dong, Y. Ma, J. C. Woicik, and D. R. Meuller, Phys. Rev. B **48**, 1918 (1993).

[4] P. D. Johnson and Y. Ma, Phys. Rev. B **49**, 5024 (1994).

[5] Y. Ma, K. E. Miyano, P. L. Cowan, Y. Aglitzkiy, and B. A. Karlin, Phys. Rev. Lett. **74**, 478 (1995).

[6] A. Carlisle, E. L. Shirley, E. A. Hudson, L. J. Terminello, T. A. Callcott, J. J. Jia, D. L. Ederer, R. C. C. Perera, and F. J. Himpsel, Phys. Rev. Lett. **74**, 1234 (1995).

[7] J. J. Jia, T. A. Callcott, E. L. Shirley, A. Carlisle, L. J. Terminello, A. Asfaw, D. L. Ederer, F. J. Himpsel, and R. C. C. Perera, Phys. Rev. Lett. **76**, 4054 (1996).

[8] J. Lüning, J-E. Rubensson, C. Ellmers, S. Eisebitt, and W. Eberhardt, Phys. Rev. B **56**, 13 147 (1997).

[9] Eric L. Shirley, Phys. Rev. Lett. **80**, 794 (1998).

[10] For an ARPES study on NiAl see, S.-C. Lui, J. W. Davenport, E. W. Plummer, D. M. Zehner, and G. W. Fernando, Phys. Rev. B **42**, 1582 (1990).

[11] A. Kaprolat and W. Schülke, Appl. Phys. A: Mater. Sci. Process. **65A**, 169 (1997).

[12] See, for example, M. Blume, J. Appl. Phys. **57**, 3615 (1985).

[13] Y. Ma, Phys. Rev. B **49**, 5799 (1994).

[14] C.-O. Almbladh, Phys. Rev. B **10**, 4343 (1977).

[15] M. van Veenendaal and P. Carra, Phys. Rev. Lett. **78**, 2839 (1997).

[16] T. Åberg, Phys. Rev. A **4**, 1735 (1971).

[17] J. Pirenne and P. Longe, Physica (Amsterdam) **30**, 277 (1964).

[18] P. Blaha, K. Schwarz, and J. Luitz, WIEN97, Vienna University of Technology, Vienna, 1997, updated version of P. Blaha, K. Schwarz, P. Sorantin, and S. B. Trickey, Comput. Phys. Commun. **59**, 399 (1990).